

See discussions, stats, and author profiles for this publication at: <https://www.researchgate.net/publication/221720122>

One-Pot Synthesis of Ag@TiO₂ Core–Shell Nanoparticles and Their Layer-by-Layer Assembly

ARTICLE *in* LANGMUIR · JANUARY 2000

Impact Factor: 4.46 · DOI: 10.1021/la991212g

CITATIONS

243

READS

511

6 AUTHORS, INCLUDING:



Isabel Pastoriza-Santos

University of Vigo

146 PUBLICATIONS 9,071 CITATIONS

SEE PROFILE



Giersig Michael

Freie Universität Berlin

289 PUBLICATIONS 16,690 CITATIONS

SEE PROFILE



Nicholas Kotov

University of Michigan

445 PUBLICATIONS 27,036 CITATIONS

SEE PROFILE

One-Pot Synthesis of Ag@TiO₂ Core–Shell Nanoparticles and Their Layer-by-Layer Assembly

Isabel Pastoriza-Santos,[‡] Dmitry S. Koktysh,[†] Arif A. Mamedov,[†]
Michael Giersig,[§] Nicholas A. Kotov,^{*,†} and Luis M. Liz-Marzán^{*,‡}

Department of Chemistry, Oklahoma State University, Stillwater, Oklahoma 74078,
Departamento de Química Física, Universidade de Vigo, E-36200 Vigo, Spain, and
Hahn-Meitner-Institut, Abteilung Physikalische Chemie, Glienickestrasse 100,
D-15109, Berlin, Germany

Received September 14, 1999. In Final Form: December 3, 1999

Silver nanoparticles coated with a uniform, thin shell of titanium dioxide are synthesized via a remarkably simple one-pot route, where the reduction of Ag⁺ to Ag⁰ and the controlled polymerization of TiO₂ on the surface of silver crystallites take place simultaneously. The prepared dispersions of coated nanoparticles display a surface plasmon band, which is significantly red-shifted with respect to that of bare Ag. High-quality ultrathin films of the core–shell clusters are prepared via layer-by-layer assembly. The nanoparticles are arranged in closely packed layers interlaced with polyelectrolyte producing a stratified core–shell hybrid material with unique structure and catalytic and electron-transport properties.

Introduction

Dispersions of nanoparticles afford accurate tuning of optical, electrical, and magnetic properties of many types of inorganic solids previously unattainable by classical synthetic means. Nanostructured materials with a characteristic dimension of structural units of 1–100 nm represent one of the most dynamic areas of modern science. Coating of semiconductor, metal, or metal oxide nanoparticles with a thin layer of a compatible material makes possible the control of interparticle and particle–matrix interactions, thereby further improving functional properties of devices on their basis and expanding the range of potential applications. The core–shell geometry has previously allowed for the enhancement of luminescence of semiconductor nanoparticles,^{1–4} preparation of bioconjugates,^{5,6} chemical and colloidal stability,^{7,8a} charging of metal cores,^{8b} and optimization of magnetic properties of nanoparticles.⁹

In the most interesting and practically promising ideas for metal sulfide/oxide clusters, for instance, light emitting diodes,^{10–13} photovoltaic elements and energy conver-

sion,^{14–16} sensors,¹⁷ memory devices,⁹ and others, the nanoparticles are utilized in the form of thin films deposited on suitable substrates. The stage of processing of the original dispersions to thin films can drastically affect the performance of the devices because of particle aggregation, phase separation, and pinhole formation. The layer-by-layer (LBL) assembly, initially developed for pairs of oppositely charged polyelectrolytes,^{18,19} has been recently applied to the preparation of nanoparticle thin films.^{9,25,26} It allows for the deposition of homogeneous, robust films with accurately controlled layer thickness and interlayer separation. Other advantages also include the hybrid organic–inorganic nature of the produced coatings, universality with regard to both substrate and material to be deposited, as well as ease of implementation.

In this communication, we report on the preparation of hybrid materials for which the simplicity of layering is combined with simplicity of the synthesis of the core–shell particles. A novel nanostructured system composed of silver cores coated by a 1–2 nm layer of titanium dioxide is produced by simultaneous reduction of silver and condensation of titanium butoxide. After adjustment of the surface charge, high-quality stratified films of the nanoparticles have been produced by the layer-by-layer assembly technique. Besides the extension of the LBL technique to the assembly of core–shell particles, which permits preparation of materials that can hardly be

[†] Oklahoma State University, kotov@okstate.edu.

[‡] Universidade de Vigo, lmarzan@cozmo.uvigo.es.

[§] Hahn-Meitner-Institut.

(1) Dabbousi, B. O.; Rodriguez-Viejo, J.; Mikulec, F. V.; Heine, J. R.; Mattoussi, H.; Ober, R.; Jensen, K. F.; Bawendi, M. G. *J. Phys. Chem. B* **1997**, *101*, 9463–9475.

(2) Danek, M.; Jensen, K. F.; Murray, C. B.; Bawendi, M. G. *Chem. Mater.* **1996**, *8*, 173–180.

(3) Peng, X. G.; Schlamp, M. C.; Kadavanich, A. V.; Alivisatos, A. P. *J. Am. Chem. Soc.* **1997**, *119*, 7019–7029.

(4) Hines, M. A.; Guyot-Sionnest, P. *J. Phys. Chem.* **1996**, *100*, 468.

(5) Bruchez, M., Jr.; Moronne, M.; Gin, P.; Weiss, S.; Alivisatos, A. P. *Science* **1998**, *281*, 2013–2016.

(6) Chan, W. C. W.; Nie, S. *Science* **1998**, *281*, 2016–2018.

(7) Correa-Duarte, M. A.; Giersig, M.; Liz-Marzán, L. M. *Chem. Phys. Lett.* **1998**, *286*, 497–501.

(8) (a) Pastoriza-Santos, I.; Liz-Marzán, L. M. *Langmuir* **1999**, *15*, 948–951. (b) Ung, T.; Liz-Marzán, L.; Mulvaney, P. *J. Phys. Chem.* **1999**, *103*, 6770–6773.

(9) Aliev, F.; Correa-Duarte, M.; Mamedov, A.; Ostrander, J. W.; Giersig, M.; Liz-Marzán, L. M.; Kotov, N. *Adv. Mater.* **1999**, *11*, 1006–1010.

(10) Colvin, V. L.; Schlamp, M. C.; Alivisatos, A. P. *Nature* **1994**, *370*, 354–357.

(11) Yang, Y.; Huang, J. M.; Yang, B.; Liu, S. Y.; Shen, J. C. *Synth. Met.* **1997**, *91*, 347–349.

(12) Schlamp, M. C.; Peng, X. G.; Alivisatos, A. P. *J. Appl. Phys.* **1997**, *82*, 5837–5842.

(13) Mattoussi, H.; Radzilowski, L. H.; Dabbousi, B. O.; Thomas, E. L.; Bawendi, M. G.; Rubner, M. F. *J. Appl. Phys.* **1998**, *83*, 7965–7974.

(14) Kronik, L.; Ashkenasy, N.; Leibovitch, M.; Fefer, E.; Shapira, Y.; Gorer, S.; Hodes, G. *J. Electrochem. Soc.* **1998**, *145*, 1748–1755. Fogg, D. E.; Radzilowski, L. H.; Dabbousi, B. O.; Schrock, R. R.; Thomas, E. L.; Bawendi, M. G. *Macromolecules* **1997**, *30*, 8433–8439. Gaponik, N. P.; Sviridov, D. V. *Ber. Bunsen-Ges. Phys. Chem.* **1997**, *101*, 1657–1659.

(15) Greenham, N. C.; Peng, X. G.; Alivisatos, A. P. *Phys. Rev. B: Condens. Matter* **1996**, *54*, 17628–17637.

(16) Alivisatos, A. P. *J. Phys. Chem.* **1996**, *100*, 13226–13239.

(17) Mussig, S.; Kotov, N. A. Unpublished results.

(18) Decher, G. *Science* **1997**, *277*, 1232–1237.

(19) Lvov, Y.; Decher, G.; Haas, H.; Möhwald, H.; Kalachev, A. *Physica B* **1994**, *198*, 89–91.

obtained by other methods, the motivation behind this work comes from the possibility of utilizing them as novel catalytic and charge storage media. Effect of the presence of titanium oxide shell and particle packing on the electron percolations in the film is within the scope of our future work.

Results and Discussion

1. Synthesis of Ag@TiO₂. The preparation of Ag@TiO₂ core-shell nanoparticles can be considered as a combination of two processes that occur sequentially in a single reaction mixture—the formation of the silver core and the coating. We have recently reported on the ability of *N,N*-dimethylformamide (DMF) to reduce silver ions and yield stable silver colloids, in the presence of a stabilizer.⁸ On the other hand, controlled hydrolysis and condensation of Ti(OC₄H₉)₄ (TOB) can be accomplished by refluxing in the presence of a chelating agent, such as acetylacetone, to slow the hydrolysis.²⁰ As a result, titania colloids with different particle sizes can be obtained. In this study, we attempted to combine these two procedures in one single procedure, comprising the high-temperature reduction of Ag⁺ by a DMF/ethanol mixture in the presence of TOB and acetylacetone.

The starting reaction mixture is prepared from two solutions.²¹ The first solution contains equimolar amounts of TOB and acetylacetone in ethanol in a concentration of 5.75 mM for each of both components. Sonication in a standard ultrasound bath for a few minutes is required to obtain a clear mixture. The second solution is 3.8 mM AgNO₃ and 0.8 M H₂O in DMF. Freshly prepared 20 mL of the first solution and 5 mL of the second one are mixed in a round-bottom beaker and stirred while heating at a reflux temperature. After 90 min, the colloid attains a green-black coloration. This stable dispersion in DMF/ethanol can be diluted with water without signs of aggregation for a period of at least 1 week (acidic pH) to 1 day (basic pH).

The prepared nanoparticles were characterized by high-resolution transmission electron microscopy (HRTEM).²² Two different populations were found on the carbon-coated copper grids, as shown in Figure 1. There is a population of larger silver particles with an average diameter of ca. 20 nm, which are homogeneously coated with a thin shell of amorphous TiO₂ as identified by EDAX. Additionally, smaller silver particles are also present on the grid, with an average particle size of some 4 nm. For them, the low contrast of the image does not allow for the visualization of a shell. However, the stability of these dispersions at pH > 2, when standard naked silver colloids flocculate, suggests that their surface is also modified by TOB.

UV-visible spectroscopy of the dilute aqueous sol of the core-shell nanoparticles shows a large red-shift of the silver plasmon band from 400 nm, which is typical for uncoated silver nanoparticles, to 435 nm, as well as largely enhanced absorbance at lower wavelengths. Both of these spectral features are related to the high refractive index of TiO₂^{23,24} being in contact with the silver surface.

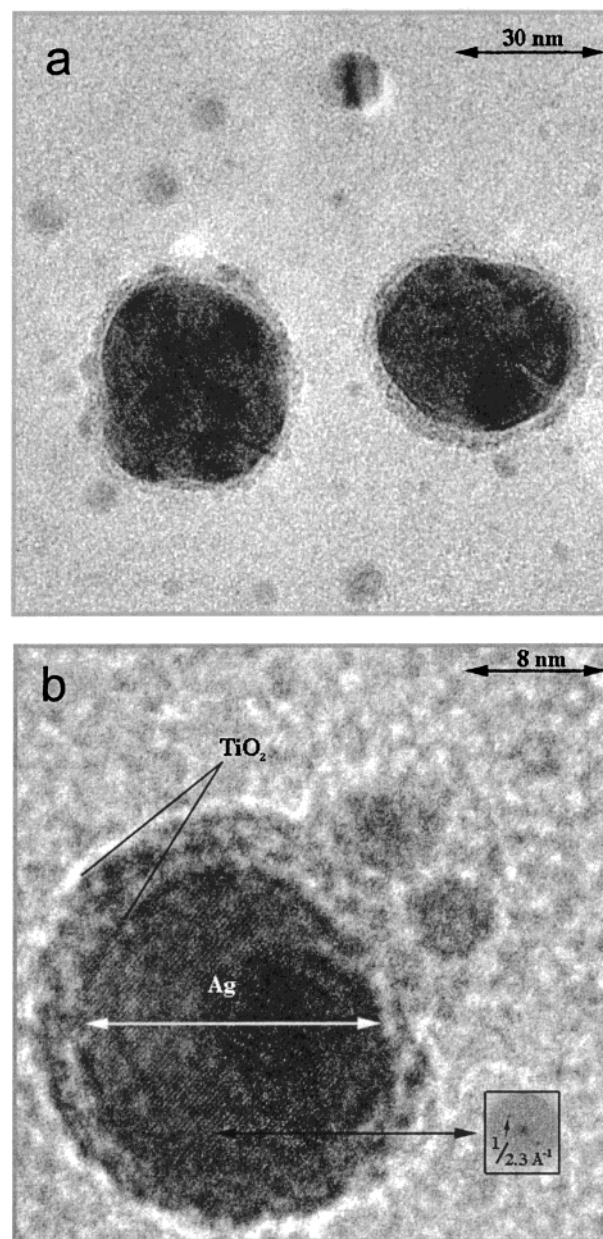


Figure 1. (a) TEM micrograph of Ag nanoparticles. Two different populations exist in the sample. The titania shell around the larger particles can be clearly seen in the images. (b) HRTEM of Ag@TiO₂ showing the crystalline nature of the metallic core and the amorphous nature of the shell.

2. Layer-by-Layer Assembly. The preparation of thin films of the core-shell nanoparticles was achieved by the layer-by-layer deposition with a polyelectrolyte.^{25–28} In this method, a monolayer of polyelectrolyte is deposited on a hydrophilic substrate. Subsequently, it is exposed to a colloidal dispersion of oppositely charged particles. The combination of both electrostatic and hydrophobic interactions²⁹ results in a strong adsorption of the nanoparticles onto the polyelectrolyte layer, while high surface charge

(20) (a) Socolan, E.; Sanchez, C. *Chem. Mater.* **1998**, *10*, 3217–3223. (b) Hanprasopwattana, A.; Srinivasan, S.; Sault, A. G.; Datye, A. K. *Langmuir* **1996**, *12*, 3173–3179.

(21) All starting chemicals in this work were purchased from Aldrich and used as received.

(22) TEM images were taken in a Phillips CM-12 instrument operating at an acceleration voltage of 120 kV, equipped with a high-resolution lens and 9800 EDAX analyzer. High-resolution images were digitally recorded with a CCD camera.

(23) Liz-Marzán, L. M.; Giersig, M.; Mulvaney, P. *Langmuir* **1996**, *12*, 4329–4335.

(24) Mulvaney, P. *Langmuir* **1996**, *12*, 788.

(25) Gao, M. Y.; Richter, B.; Kirstein, S.; Möhwald, H. *J. Phys. Chem. B* **1998**, *102*, 4096–4103.

(26) Kotov, N. A.; Dekany, I.; Fendler, J. H. *J. Phys. Chem.* **1995**, *99*, 13065–13069.

(27) Kotov, N. A.; Haraszti, T.; Turi, L.; Zavala, G.; Geer, R. E.; Dekany, I.; Fendler, J. H. *J. Am. Chem. Soc.* **1997**, *119*, 6821–6832.

(28) Liu, Y. J.; Wang, A. B.; Claus, R. *J. Phys. Chem. B* **1997**, *101*, 1385–1388.

(29) (a) Kotov, N. A. *Nanostruct. Mater.* **1999**, *12*, 789–796. (b) Mamedov, A. A.; Ostrander, J. W.; Kotov, N. To be published.

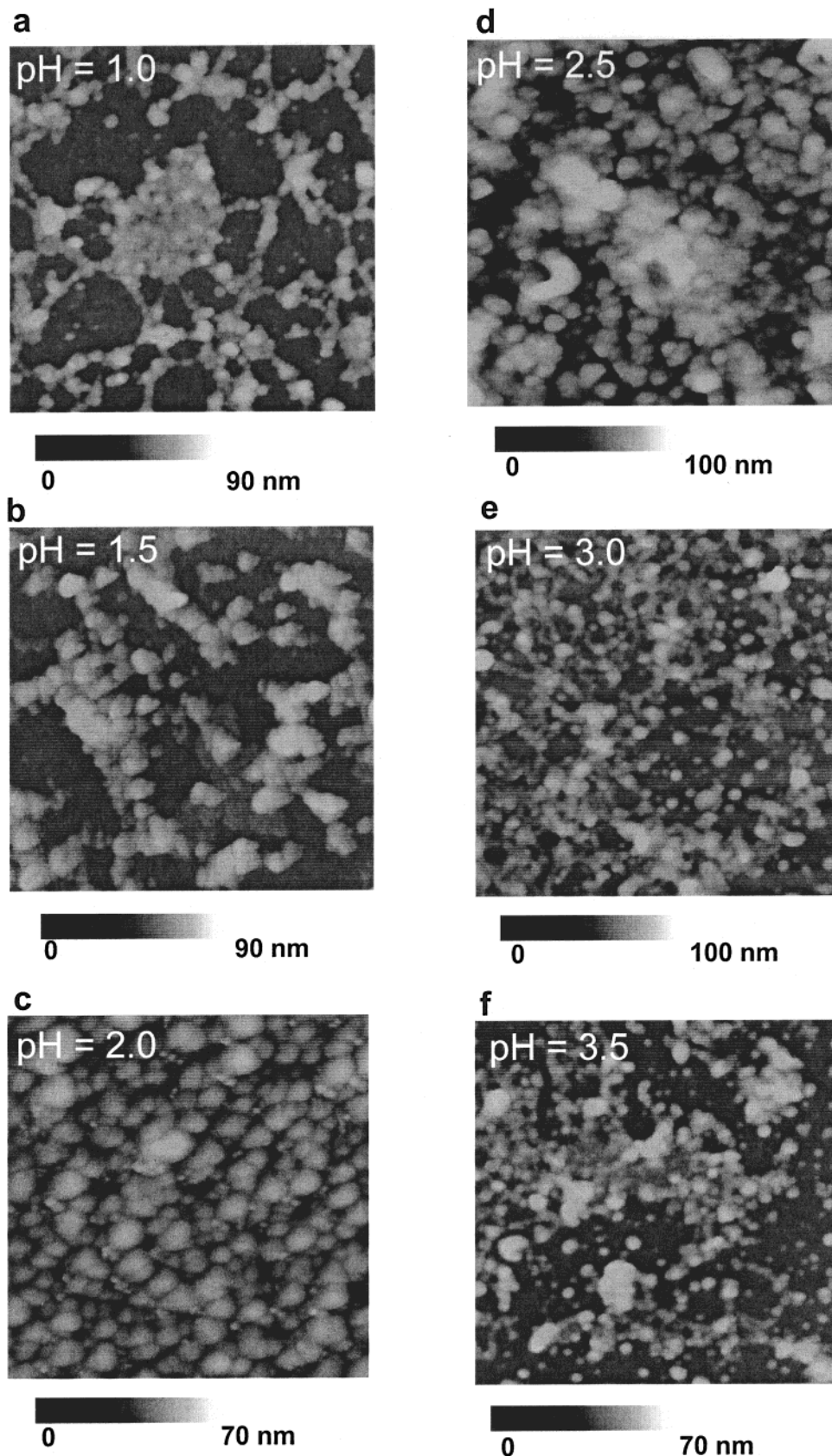


Figure 2. $1\ \mu\text{m} \times 1\ \mu\text{m}$ AFM images of monolayers of the nanoparticles shown in Figure 1 assembled from dispersions at pH = 1.0 (a), 1.5 (b), 2.0 (c), 2.5 (d), 3.0 (e), and 3.5 (f). In (c) the two populations of nanoparticles seen in Figure 1 can be identified.

prohibits the formation of thick, rough films. The thickness and lateral particle density of the films can be varied by changing the strength of electrostatic and hydrophobic interactions.^{29a}

A relatively hydrophobic environment of the DMF–ethanol mixture of the original dispersion and low surface charge of nanoparticles makes the LBL from the as prepared dispersions problematic. Therefore, the first step

for the film preparation is the 1:15 dilution of the original dispersion (in DMF/ethanol) with water at pH < 3.5.³⁰ Under these conditions, the titania-coated particles become positively charged, while the large amount of dilution water activates the hydrophobic attraction to the polyelectrolyte strands. For positively charged Ag@TiO₂ nanoparticles, negatively charged poly(acrylic acid), $M_w = 100\,000$ (PAA) is used as a partner polyelectrolyte for LBL.

The actual deposition procedure on silicon wafers or glass substrates starts from a 5 min exposure of a Si wafer (glass slide) to a 0.5 wt % solution of high molecular weight poly(dimethyldiallylammonium chloride), $M_w = 400\,000$ –500 000 (PDDA) at pH = 3.6.³¹ The positively charged PDDA adsorbs on a negatively charged silicon oxide surface layer producing a foundation layer, which ensures the charge uniformity of the underlying surface of the substrate. After 30 s of washing in two separate beakers with deionized water (18 M Ω), the PDDA-primed substrate is dipped into a 1 wt % solution of PAA at pH > 3.5, which changes the surface charge to negative. Following the same washing procedure, the substrate is exposed to positively charged Ag@TiO₂ nanoparticles in the diluted dispersion described above for 60 min. After being rinsed with water and dried with a stream of nitrogen, the film of core-shell nanoparticles is analyzed by atomic force microscopy (AFM).

The AFM images reveal that the surface density of nanoparticles can be varied by changing the pH of the nanoparticle dispersions (Figure 2). The best ordering is observed at pH = 2.0, when the nanoparticles form fairly closely packed films (Figure 2c). A deviation in pH in both directions from the optimal range pH = 2.0–2.5 yields deterioration in particle ordering. At low pH ≤ 2.0 , the adsorption of protons on the TiO₂ shells results in a high surface charge of nanoparticles (IEP of TiO₂ is pH = 6.5–5.2³²). Consequently, strong repulsion between them dominates over other intermolecular forces. Additionally, the degree of PAA ionization is decreased, too. Both factors make adsorption thermodynamically less favorable and rarified layers of individual nanoparticles are produced (Figure 2a,b). At pH = 2.0, the surface charge of nanoparticles is decreased and so is the interparticle repulsion. The relative contribution of the electrostatic and hydrophobic attraction to the PAA-coated surface increases, which results in increase of particle density. The situation when the repulsion and attraction both remain strong, while balancing each other, promotes uniformly disperse structures as can be seen in Figure 2c. Further increase of pH to 2.5 leads to shift of the balance toward nonspecific attractive interactions due to the charge independent hydrophobic interactions of nanoparticles with each other and with PAA macromolecules. In response to that, the films become thicker and less organized with fairly large aggregates distributed all over the surface (Figure 2d). At relatively high pH (≥ 3.0), the kinetics of adsorption becomes very slow due to smaller charge on TiO₂ and the corresponding weakness of the long-range electrostatic attraction of nanoparticles to the substrate, which results in rarified films consisting from 3D clusters of many

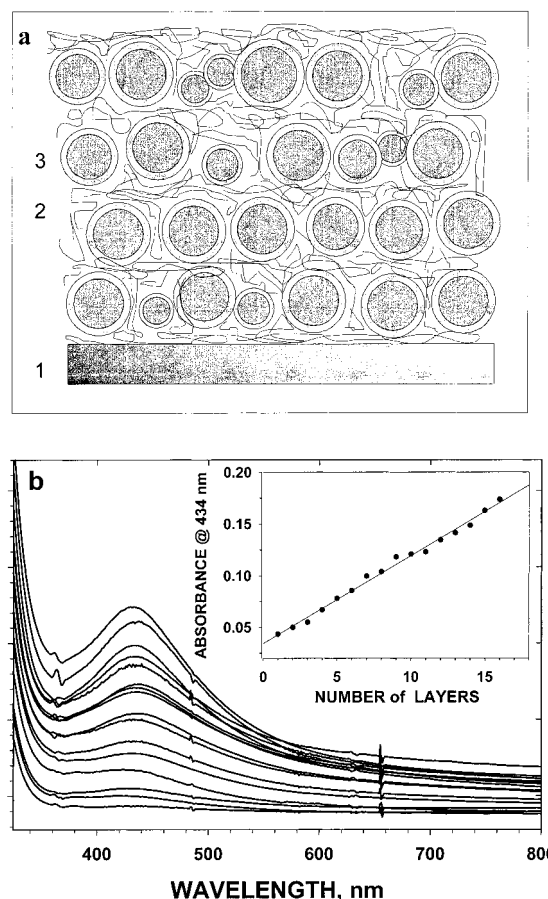


Figure 3. (a) Schematic representation of the layer-by-layer assembled nanoparticulate film. (b) UV-vis spectra of sequentially adsorbed Ag@TiO₂/PAA bilayers assembled at pH = 2.5. The inset shows the dependence of absorbance at 434 nm vs the number of deposition cycles.

particles (Figure 2e,f). Notably, the agglomeration patterns of the nanoparticles transform as pH changes (compare panels a and f of Figure 2). This fact is also indicative of the changes in the nature of interparticle and particle/polyelectrolyte interactions. Adding further to the complexity of the process and to the factors that control the ordering in such systems is the presence loose segments of polyelectrolyte chains protruding into the solution, which change their conformation with pH. They are suspected to stimulate the particle aggregation during the adsorption process.³³

Good surface coverage and alternation of the surface charge for layers of nanoparticles and polyelectrolyte make possible the cyclic repetition of the dipping procedure. This feature can be used to build up multilayers of nanoparticles interlaced with polyelectrolyte (Figure 3a). This process of multilayer buildup on glass slides can be monitored by UV-visible spectroscopy (Figure 3b). The consecutively acquired spectra display a virtually linear increase of absorbance in every deposition cycle (i.e., with each PAA/Ag@TiO₂ double layer). Such behavior is commonly observed for many LBL deposited systems.^{25–28,34–37}

(30) Water was purified by a Millipore Milli-Q system (18 M Ω). Acidity of water used for dilution of the DMF/ethanol dispersion was adjusted with dilute HCl.

(31) Glass substrates and silicon wafers were cleaned by piranha solution (a mixture of 30% H₂O₂ and concentrated H₂SO₄ 1:3 v/v) for 5 min at room temperature followed by washing with deionized running water.

(32) Macdonald, D. E.; Markovic, B.; Boskey, A. L.; Somasundaran, P. *Colloids Surf., B* **1998**, *11*, 131–139. Szymczyk, A.; Fievet, P.; Reggiani, J. C.; Pagetti, J. *Desalination* **1998**, *115*, 129–134.

(33) Correa-Duarte, M. A.; Giersig, M.; Kotov, N. A.; Liz-Marzan, L. *Langmuir* **1998**, *14*, 6430–6435.

(34) Lvov, Y.; Ariga, K.; Onda, M.; Ichinose, I.; Kunitake, T. *Langmuir* **1997**, *13*, 6195–6203.

(35) Decher, G.; Schmitt, J.; Brand, F.; Lehr, B.; Oeser, R.; Losche, M.; Bouwman, W.; Kjaer, K.; Calvert, J.; Geer, R.; Dressik, W.; Shashidhar, R. *Adv. Mater.* **1998**, *10*, 338–341.

(36) Baur, J. W.; Kim, S.; Balanda, P. B.; Reynolds, J. R.; Rubner, M. F. *Adv. Mater.* **1998**, *10*, 1452–1455.

It demonstrates a degree of vertical ordering of the multilayers. Importantly, the layer-by-layer character of the deposition procedure affords thickness control of the film with an accuracy equal to the thickness of one particle layer. Note that the position of the surface plasmon band at 434 nm of silver remains identical to that of the sol, which indicates that, while being in close contact with each other, the nanoparticles remain electrically insulated. This feature distinguishes the proposed films from LBL assemblies of naked silver clusters.^{38,39} Such an effect should be attributed to the presence of an insulating (probably amorphous) shell of titania around the metal cores. It impedes electron exchange between them, typically manifesting in the red-shifted plasmon peak.

(37) Cassagneau, T.; Mallouk, T. E.; Fendler, J. H. *J. Am. Chem. Soc.* **1998**, *120*, 7848–7859.

(38) Mulvaney, P.; Liz-Marzán, L. M.; Giersig, M.; Ung, T. *J. Mater. Chem.*, in press.

(39) Schrof, W.; Rozouvan, S.; Vankeuren, E.; Horn, D.; Schmitt, J.; Decher, G. *Adv. Mater.* **1998**, *10*, 338–341.

In summary, we have shown that the simultaneous reduction of silver salts and hydrolysis of titanium alkoxides can lead to stable dispersions of titania-coated silver nanoparticles, which can be subsequently transferred into water. The coated particles can be easily deposited as densely packed mono- or multilayers of uniform thickness. The study of the catalytic and electron-transport properties of these films will be reported elsewhere.

Acknowledgment. The authors thank reviewers for helpful comments. L.M.L.M. acknowledges the support from the Spanish Xunta de Galicia (Project No. PGIDT-99PXI30104B and personal travel fellowship). N.A.K. thanks NSF CAREER (CHE-9876265), AFOSR, NATO (CRG 971167), OSU Sensor Center, and Nomadics, Inc., for the partial financial support of this research. D.S.K. acknowledges support from the NSF/NATO (NSF-NATO Grant No. DGE-9902637) for the postdoctoral fellowship.

LA991212G